Research Article

Steam Explosion Extraction of Pectin from Watermelon Rinds: Identification of Integrated Crystalline Mineral Phases and Thermal Characterization

Thanita Bilman and Nantharat Phruksaphithak*
Faculty of Science and Digital Innovation, Thaksin University, Phatthalung, Thailand
Centre of Excellence for Agricultural Innovation and Bioproducts of Thaksin University, Thaksin University, Phatthalung, Thailand

Nattiyaporn Na nakorn, Kornkanok Meesen, Sudsakhorn Singthong and Visit Boonchom
Faculty of Science and Digital Innovation, Thaksin University, Phatthalung, Thailand

* Corresponding author. E-mail: nantharat@tsu.ac.th DOI: 10.14416/j.asep.2026.08.018
Received: 16 February 2026; Revised: 17 March 2026; Accepted: 17 April 2026; Published online: 31 August 2026

Abstract
This study explores the potential of utilizing watermelon rinds, a significant agricultural byproduct, as a sustainable source for pectin extraction using the steam explosion (SE) technique at 121 °C for 30 min. The SE-extracted watermelon pectin (WP) was characterized and compared with standard commercial citrus pectin (CP). The WP exhibited an extraction yield of 3.41 ± 0.13%, a degree of esterification (DE) of 37.42 ± 1.92%, and a methoxyl content of 6.10 ± 0.20%, classifying it as a low-methoxyl pectin. FTIR analysis confirmed the preservation of characteristic pectin functional groups. Notably, XRD patterns revealed that while CP was predominantly amorphous, WP contained co-extracted crystalline mineral phases. SEM-EDS and high-resolution elemental mapping verified that these phases, consisting of Sylvite (KCl), Calcite ($CaCO_3$), and Halite (NaCl), were homogeneously integrated and securely embedded throughout the pectin biopolymer matrix. These findings were consistent with the significantly higher ash content (6.42 ± 0.15%) and thermal residue (43.83% at 550 °C) observed in WP than in CP. DSC analysis indicated distinct thermal phase transitions, characterized by a major endothermic dehydration peak at 135.85 °C. SEM observations confirmed that SE effectively disrupted the cell wall matrix, yielding a porous pectin network with integrated mineral microparticles. These results demonstrate that steam explosion is a promising alternative that is potentially greener than conventional acid extraction due to reduced chemical and acid consumption for producing functional pectin with co-extracted and integrated crystalline mineral phases, offering viable potential for application in functional food systems.

Keywords: Low-methoxyl pectin, Pectin extraction, Physicochemical properties, Steam explosion, Thermal stability, Watermelon rind

1 Introduction

Watermelon is among the most widely cultivated fruits globally, with production reaching approximately 99.7 million tons in 2023 [1]. However, the fruit suffers from a high waste rate of about 45% due to its short shelf life and the non-consumption of its rinds, which represent 30-40% of the total fruit weight [1], [2]. This leads to millions of tons of discarded biomass annually, posing a significant environmental challenge [3] as these rinds are often dumped without industrial application [2]. Recently, research has pivoted towards transforming these zero-value wastes into sustainable food ingredients and value-added products, such as 3D-printed functional gummies and biodegradable preservation films [4]. The valorization of such agricultural byproducts through advanced biorefining technologies has gained widespread attention within circular and sustainable green economic frameworks [5]. Various biomass pretreatment methodologies, combining physical and chemical actions, have been continuously developed to disrupt rigid plant cell wall barriers and maximize the recovery of high value biopolymeric structures [6].

Watermelon rinds are particularly rich in bioactive compounds and structural polysaccharides, especially pectin, which serves as a high-value functional biopolymer in the food, pharmaceutical, and cosmetic industries [7], [8]. Beyond pectin, watermelon rinds are also abundant in essential minerals, including potassium (130.04 mg/100g), sodium (515.44 mg/100g), and calcium (311.22 mg/100g) [2], [9]. Unlike conventional pectin extraction, where mineral components typically remain as discarded ash residues, appropriate processing methods can securely integrate these naturally occurring mineral phases into the final biopolymer framework, offering a distinctive structural profile and beneficial functional traits for downstream applications[2], [7], [8].

Pectin, a complex polysaccharide primarily composed of homogalacturonan, rhamnogalacturonan I, and rhamnogalacturonan II motifs with neutral sugars [8], features D-galacturonic acid units linked by α-(1→4) glycosidic bonds in its backbone, which can be partially methylated or acetylated. Its emulsifying properties are influenced by the extraction method and source [7]. Various methodologies have been explored for pectin extraction, including subcritical water, pressurized natural deep eutectic solvents, and steam explosion, with attention to parameters like temperature affecting molecular weight and polydispersity [10]. Conventional extraction often involves prolonged heating with strong mineral acids, raising environmental concerns and risking pectin degradation [7], [8].

Steam explosion (SE) represents a promising pretreatment technology that is potentially greener than conventional acid extraction, owing to the significantly reduced consumption of harsh chemicals and acids, by subjecting biomass to high-pressure saturated steam followed by rapid decompression [10]. This process effectively disrupts the lignocellulosic matrix, enhancing pectin accessibility and reducing processing times compared to conventional acid hydrolysis [10], [11].

Despite the potential of SE, comprehensive data on how extraction parameters affect the structural and thermal properties of pectin from watermelon rinds remain limited [8]. While studies have examined acid hydrolysis and microwave-assisted extraction from this waste [8], [12], detailed FTIR patterns, thermal profiles via TGA/DSC, and other characterizations specific to SE-extracted watermelon pectin are scarce [1], [7]. This study addresses this gap by extracting pectin from watermelon rinds via steam explosion and comprehensively characterizing its physicochemical properties, functional groups (including the degree of esterification and methoxyl content), crystallinity, elemental composition, distribution pathways, thermal stability, and morphology using FTIR, XRD, TGA, DSC, and SEM-EDS with high resolution elemental mapping, alongside its water holding capacity. These insights successfully demonstrate the feasibility of SE for sustainable pectin production from watermelon waste, elucidating complex structure composition-function relationships of the recovered biopolymer matrix for potential industrial applications.

2 Materials and Methods

2.1 *Material*

Watermelon rinds were collected from local markets in Phatthalung, Thailand. The rinds were washed, separated from the red flesh, and sliced into small pieces. The prepared rinds were dried in a hot air oven at 60 °C until a constant weight was achieved, then ground into powder and sieved through a 60-mesh screen. Commercial citrus pectin (CP, Grade ADC102, China) obtained from Lanagrow Chemical (Thailand) was used as a reference material. All chemical reagents used in this study were of analytical grade.

2.2 *Pectin extraction via steam explosion*

The extraction was performed using a steam explosion system. Briefly, the watermelon rind powder was mixed with distilled water at a 1:12 w/v solid-to-liquid ratio. The mixture was placed in the reaction chamber and subjected to saturated steam at 121 °C for 30 min. Following the treatment, the pressure was instantaneously released to atmospheric pressure. The resulting slurry was filtered, and the filtrate was mixed with 80% ethanol (1:2 v/v) to precipitate the pectin. The precipitate was collected, washed with ethanol, and dried at 50 °C to obtain the extracted pectin powder. The extraction yield was calculated following Equation (1).

$$Extract\ yield\ (\%) = \frac{W_1}{W_2} \times 100 \quad (1)$$

where W_1 is the weight of the extracted dry pectin (g) and W_2 is the weight of the initial dry watermelon rind powder (g).

2.3 *Physicochemical characterization*

The physicochemical properties of both the WP and CP were determined in triplicate to ensure accuracy.

2.3.1. Moisture content

The moisture content of the extracted WP and commercial CP was determined by drying the samples in a hot air oven at 105 °C until a constant weight was achieved [13]. The moisture content percentage was calculated using Equation (2).

$$Moisture\ Content\ (\%) = \frac{W_3 - W_4}{W_3} \times 100 \quad (2)$$

Where W_3 is the weight of pectin before drying (g) and W_4 is the weight of pectin after drying(g).

2.3.2 Ash content

The dried samples from the moisture analysis were placed in a muffle furnace and incinerated at 550 °C for 5 hours [14] until the residues turned into white or light grey ash [15]. Ash content of pectin was determined in triplicate. The ash percentage was determined gravimetrically relative to the initial dry sample weight as in Equation (3).

$$Ash\ Content\ (\%) = \frac{W_6}{W_5} \times 100 \quad (3)$$

Where W_6 is the weight of the ash (g) and W_5 is the weight of the dry pectin sample before ashing (g).

2.3.3. *Water holding capacity*

The water holding capacity (WHC) was measured using the centrifugation method modified from Duggal [16]. Briefly, 0.05 g of the pectin sample was dispersed in 2 mL of distilled water in a pre-weighed centrifuge tube. The suspension was stirred thoroughly and allowed to hydrate at room temperature for 24 h to ensure complete saturation. Subsequently, the mixture was centrifuged at 4,000 rpm for 20 min. The supernatant was carefully decanted, and the tube containing the wet pectin pellet was weighed. The WHC was calculated as the mass of retained water per gram of dry pectin using Equation (4).

$$WHC\ (gH_2O/gPectin) = \frac{W_8 - W_7}{W_7} \quad (4)$$

Where W_8 is the weight of the wet pectin after decanting the excess water (g) and W_7 is the initial weight of the dry pectin sample (g)

2.3.4 Molecular weight

The average molecular weight (M_w) of the pectin samples was determined based on the relationship between intrinsic viscosity and polymer chain length using the Mark-Houwink-Sakurada equation [17], [18]. Viscometric measurements were performed using an Ubbelohde capillary viscometer at a controlled temperature of 25.0 ± 0.1 °C. To prepare the sample, 0.1 g of dried pectin was dissolved in 100 mL of 0.1 mol/L NaCl solution, which serves to suppress electro-viscous effects. The mixture was stirred gently and allowed to equilibrate for 12 h before being filtered through a 0.45 µm membrane. A 15 mL aliquot of the filtered solution was introduced into the viscometer. Upon reaching thermal equilibrium in a thermostatic water bath, the flow times and densities were recorded. The relative viscosity (η_r) was determined according to Equation (5).

$$\eta_r = \frac{\eta}{\eta_s} = \frac{t_1 d_1}{t_2 d_2} \quad (5)$$

Where η and η_s represents the viscosities of the pectin solution and the solvent, respectively. The variables t_1 and t_2 denote the flow times (s), while d_1 and d_2 correspond to the densities (g/cm³). Subsequently, the intrinsic viscosity [η] (L/g) was calculated using the following relationship (Equation (6)).

$$[\eta] = \frac{\sqrt{2(\eta_{sp} - \ln \eta_r)}}{C} \quad (6)$$

Where C is the pectin concentration (g/L) and η_{sp} is the specific viscosity (η_r - 1). Finally, the M_w was estimated via the Mark-Houwink-Sakurada equation as shown in Equation (7).

$$[\eta] = k\,[M_w]^a \quad (7)$$

In this system, the constants k and α were defined as 4.36×10^{-5} L/g and 0.78, respectively, which are specific for pectin in a 0.1 mol/L NaCl solvent at 25 °C [18].

2.4 *Instrumental analysis*

2.4.1 FTIR spectroscopy

The FTIR spectra of the extracted pectin samples were measured using an FTIR spectrophotometer (Agilent Cary 630 FTIR Spectrometer, USA). The spectra were recorded in the wavelength range of 4000 to 650 cm^{-1} in attenuated total reflection (ATR) mode at a resolution of 4 cm^{-1} with 32 scans per sample. This analysis was utilized to identify the functional groups and evaluate the structural integrity of the pectin biopolymer.

The degree of esterification of the extracted pectin was determined using Fourier Transform Infrared Spectroscopy. The DE of pectin was calculated based on the relative absorbance areas under the peak corresponding to the esterified carboxyl groups and the free carboxylic acid groups [17], [19]. Specifically, the absorbance at approximately 1740 cm^{-1} (assigned to C=O stretching of ester groups) and 1626 cm^{-1} (assigned to the asymmetric stretching of carboxylate anions) was used in Equation (8).

$$DE\ (\%) = \frac{Area_{1740}}{Area_{1740} + Area_{1626}} \times 100 \qquad (8)$$

Where A_{1740} represents the area under the peak of the esterified group, and A_{1626} corresponds to the area under the peak of the free carboxylic group.

The methoxylation percentage (%MeO) of the extracted pectin was estimated based on the empirical relationship proposed by Santiago-Gomez et al. [20], which correlates the methoxyl content directly with the degree of esterification. This estimation was conducted following Equation (9)

$$MeO\ (\%) = \frac{16.32}{100} \times DE \qquad (9)$$

2.4.2. Thermal analysis

The TGA profile of the extracted pectin (6-7 mg) was investigated using a thermogravimetric analyzer (TGA-4000, PerkinElmer, USA). The analysis was conducted in a controlled environment to prevent oxidative degradation, with a heating rate of 10 °C/min over a temperature range of 25 to 600 °C [21]. This analysis allowed for the determination of mass loss stages, including moisture evaporation, the primary degradation of the galacturonic acid backbone, and the final carbonization of the organic matrix [8], [21].

DSC analysis was performed using a Netzsch DSC instrument (204 F1 Phoenix, USA). Approximately 10 mg of the dried sample was placed in a standard Indium crucible and hermetically sealed [22]. The measurement was conducted under a nitrogen atmosphere (flow rate: 10 mL/min) with a heating rate of 10 °C/min, covering a temperature range from 25 to 300 °C. An empty Indium crucible served as the Thermal transition parameters, including peak temperature (Tpeak), and enthalpy change (ΔH), were calculated from the resulting thermograms to assess the melting and crystallization behavior of the pectin biopolymer.

2.4.3 XRD analysis

The crystalline structure and phase orientation of the pectin samples were examined by X-ray Diffraction (XRD) using a Bruker D8 Advance diffractometer (Bruker AXS, Germany) equipped with Cu-Kα radiation. The diffraction patterns were recorded over a scanning range of 5° to 40° (2θ) with a step size and scanning speed appropriate for capturing the amorphous and semi-crystalline characteristics of pectic polysaccharides.

2.4.4 SEM-EDS analysis

The surface morphology of both CP and the WP was observed using a Field Emission Scanning Electron Microscope (FE-SEM, FEI Quanta 450 FEG, USA) equipped with an Energy-Dispersive X-ray Spectrometer (EDS, Oxford Instruments). Prior to high-vacuum observation, the dried samples were mounted on aluminum stubs using conductive carbon tape and sputter-coated with gold to eliminate charging effects. Concurrently, EDS spectra were collected from selected surface regions to determine the quantitative weight percentages (wt%) of carbon, oxygen, and co-extracted mineral elements (potassium(K), sodium (Na), chlorine (Cl), and calcium (Ca)). Elemental mapping was also performed to visualize the spatial distribution and integration of these crystalline mineral phases across the organic pectic biopolymer framework.

3 Results and Discussions

3.1 *Physicochemical properties and chemical composition of extracted pectin*

The physicochemical characteristics of pectin extracted from watermelon rinds using the steam explosion technique, compared with CP and standards set by the International Pectin Producers Association, are presented in Table 1.

The extraction yield was 3.41 ± 0.13%, representing efficient recovery in a short processing time (30 min) compared to conventional acid extraction methods [10]. Although slightly lower than some acid-extraction yields, the rapid decompression in SE facilitates a more sustainable process by reducing chemical and energy inputs [10].

3.1.1. Degree of esterification and methoxyl content

The watermelon rind pectin (WP) exhibited a DE of 37.42 ± 1.92%, significantly lower than commercial pectin (CP) (57.19 ± 2.90%) and confirming its classification as Low-Methoxyl Pectin (DE < 50%) [23], [24], [25]. The methoxyl content of 6.10 ± 0.20% is consistent with this classification, falling within the International Pectin Producers Association (IPPA) specified range of 2.2 - 7.8% for low-methoxyl variants. The reduced DE is a direct consequence of the SE process, in which high pressure steam followed by rapid decompression induces partial de-esterification of the polygalacturonic acid chain [10], [26]. This LMP classification confers a distinct functional advantage because, unlike High-Methoxyl Pectin (HMP), which requires high sugar concentrations (> 65%) and low pH to gel, this SE-extracted pectin can form stable gels over a wider pH range. This gelation occurs via the egg-box model with divalent cations [8], making it particularly suitable for low calorie and functional food applications.

3.1.2. Purity and mineral co-extraction

The moisture content of the SE-extracted WP was 10.33 ± 0.79%, which is within the IPPA maximum limit of 12% [7], [8], [13], indicating that the drying process was adequate. The ash content was 6.42 ± 0.15%, which also met the IPPA maximum limit of 10% [7], [13], [28], although it was higher than that of CP (2.23 ± 0.2%). The ash content of the WP is lower than the value (7.88%) reported by Mamiru [7]. Generally, a lower ash content in pectin signifies higher purity. The variation in ash content observed across different studies can be attributed to the watermelon varieties, pre-treatment methods, and specific extraction techniques employed. The higher ash content in the SE-extracted pectin compared to CP is likely due to the nature of the steam explosion process. During SE, the rapid pressure release disrupts the cell wall structure of the watermelon rind, which not only releases pectin but also allows co-extraction of inorganic minerals such as potassium and magnesium that are naturally present in watermelon rind [7], [29]. In conventional acid extraction, prolonged washing and purification steps help reduce these mineral residues, whereas the shorter processing time in SE provides less opportunity for their removal [7]. Although the ash content in this study was within the acceptable range, further purification steps may be considered to reduce it closer to levels typically seen in CP. On the other hand, the presence of these minerals may be beneficial if the extracted pectin is intended for use in nutritionally enriched food products [7].

Table 1: Physicochemical properties of CP and WP.

Sample	Yield (%)	Moisture (%)	Ash (%)	Mw (Da)	DE (%)	MeO (%)	WHC (g H_2O/g pectin)
CP	n.d	5.76 ± 0.13	2.23 ± 0.2	12826.18 ± 1026.09	57.19 ± 2.9	9.33 ± 0.21	6.23 ± 0.11
WP	3.41 ± 0.13	10.33 ± 0.79	6.42 ± 0.15	1777.90 ± 160.00	37.42 ± 1.92	6.10 ± 0.20	2.71 ± 0.15
IPPA [27]	n.d.	Max. 12%	Max. 10%	n.d.	< 50% (low methoxyl)	2.2 - 7.8 %	n.d.

Notes : n.d. = not determined

3.1.3. Molecular weight and water holding capacity

A noteworthy observation is the substantial difference in Molecular Weight (Mw). The SE-extracted pectin had an average molecular weight (Mw) of 1,777.90 ± 160.00 Da, which is significantly lower than that of the CP (12,826.18 ± 1,026.09 Da). This indicates that while SE is efficient for recovery, the high-temperature/high-pressure environment can lead to the thermal degradation or depolymerization of the pectic polysaccharides into shorter chains [10], [21]. This reduction directly correlates with the lower water holding capacity (WHC) (2.71 g H_2O/g pectin compared to that of CP (6.23 g H_2O/g pectin). Shorter chains have fewer available hydroxyl groups and a less complex network to entrap water molecules [22]. Future optimization of SE parameters (pressure and residence time) is essential to balance extraction efficiency with the preservation of molecular weight for high viscosity.

3.2 *Fourier transform infrared spectroscopy analysis*

FTIR spectroscopy was employed to identify the functional groups and structural transformations during the steam explosion extraction. The comparative spectra of raw watermelon rind, extracted pectin, and CP are illustrated in Figure 1. All three samples exhibited a broad, intense absorption band in the region of 3400 - 3300 cm^{-1}, corresponding to the O - H stretching vibrations of the galacturonic acid polymer and adsorbed water molecules [8], [17]. The peaks observed at approximately 2930 cm^{-1} are attributed to the C-H stretching of CH, CH_2 ,CH_3 and groups in the polysaccharide chains [8].

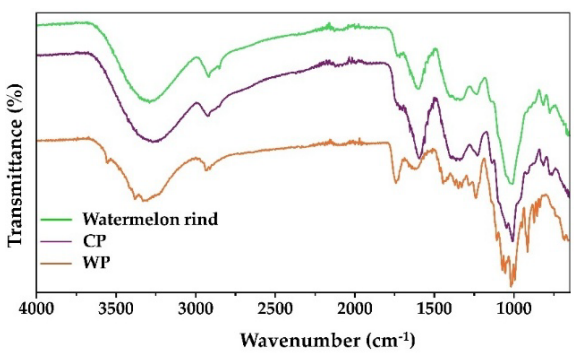

Figure 1: FT-IR spectra of raw watermelon rinds, commercial pectin (CP), and extracted watermelon pectin (WP).

3.2.1. Structural differentiation in the carbonyl region

A significant structural differentiation is observed in the carbonyl stretching region (1750 - 1600 cm^{-1}). The peak at approximately 1740 cm^{-1} is assigned to the esterified carboxyl groups (C=O), while the peak near 1620 corresponds to the free carboxylate groups (COO^-) [8], [22]. The CP spectrum shows a dominant peak at 1740 cm^{-1} relative to 1620 cm^{-1}, which is characteristic of High Methoxyl Pectin. In contrast, the extracted WP displays a more pronounced intensity at 1620 cm^{-1}. This spectroscopic evidence directly correlates with the lower Degree of Esterification (DE = 37.42 ± 1.92 %) and confirms that the steam explosion process effectively yielded Low-Methoxyl Pectin [8]. The shift in peak intensity suggests that the high temperature and high pressure conditions of SE may have induced partial de-esterification of the pectin backbone, converting ester groups into free carboxyl groups [10], [26].

3.2.2. Transformation from raw rind to extracted pectin

The spectrum of the extracted pectin shows a high degree of similarity to the raw rind in the fingerprint region (below 1500 cm^{-1}), indicating that the steam explosion technique successfully preserved the fundamental pectic backbone from the cell wall [21]. However, the peaks in the extracted pectin appear more defined and intense compared to the raw rind. This enhancement is primarily attributed to the explosive deconstruction of the complex lignocellulosic matrix, which removes interfering components like hemicellulose and lignin, thereby enriching the pectic fraction.

3.2.3. Structural integrity and glycosidic bonds

Furthermore, the absorption bands in the fingerprint region (1200 - 900 cm^{-1}), specifically around 1015 cm^{-1}, are characteristic of the glycosidic bond and the pyranose ring of the galacturonic acid backbone [8], [17]. The consistent presence of these peaks across all samples confirms that despite the physical intensity of the steam explosion method, the structural integrity of the pectin chains remained largely intact [17], [30]. This reinforces the feasibility of using SE as a green and efficient technology for recovering high-quality functional biopolymers from agricultural waste [10].

3.3 *Surface morphology analysis (SEM)*

The surface morphology of the extracted WP was examined using SEM and compared with CP to evaluate the structural impact of the steam explosion technique. As illustrated in Figure 2, the CP exhibited a relatively smooth, dense, and continuous surface with large, folded structures. This morphology is typical for highly purified pectin produced through standardized chemical extraction and refining processes, where gentle solubilization preserves a more cohesive and uniform polymeric matrix [29], [30].

In contrast, SE-extracted pectin from watermelon rinds exhibited a markedly different morphology. It featured a highly fragmented, porous, and irregular surface with visible cracks, flaky layers, and integrated spherical micro-particles [31], [32], [33]. These changes stem directly from the SE mechanism, where high-pressure steam penetrates lignocellulosic pores and is followed by rapid decompression that flashes internal moisture into steam [10].

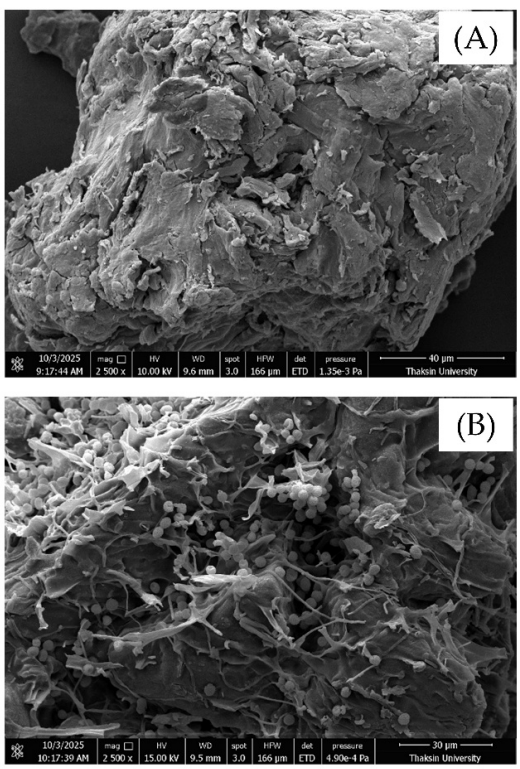

Figure 2: SEM micrographs at 2500x of (A) commercial citrus pectin (CP) and (B) watermelon pectin (WP) extracted via the steam explosion technique.

This process generates intense mechanical shear forces, shattering the compact cell wall and yielding the observed disordered structure [32]. The spherical micro-structures, absent in CP, likely arise from multiple SE-induced processes beyond mineral co-extraction. First, high-temperature/pressure conditions during SE residence time partially degrade pectic polysaccharides and hemicellulose into small carbohydrate clusters [32], [34]. Second, rapid decompression alters the thermodynamic state, prompting pectic chains to self-aggregate into spheres to minimize surface energy during cooling and drying [34]. Third, matrix disruption releases cellular components like starch granules or proteins, which integrate into the porous pectin network due to rapid extraction [8]. These distinctive features, including increased porosity and micro particles, set SE-extracted pectin apart from refined commercial types, potentially boosting effective surface area. This may improve solubility, hydration and mineral retention, aligning with the higher ash content and crystalline phases in XRD [8], [35].

3.4. *X-ray diffraction analysis*

The crystalline structure and phase orientation of the WP were evaluated using XRD and compared with CP, as illustrated in Figure 3. The XRD patterns of both samples exhibit a characteristic broad diffraction peak (halo) centered at approximately $2\theta = 14°$ and 21 - 23° [7], [36]. This broad scattering is typical of the amorphous nature of the galacturonic acid polymer chains, which are the primary structural units of pectin [7], [37]. The predominantly amorphous characteristic of both samples is significant for functional applications because a disordered molecular arrangement indicates a lack of long-range order.

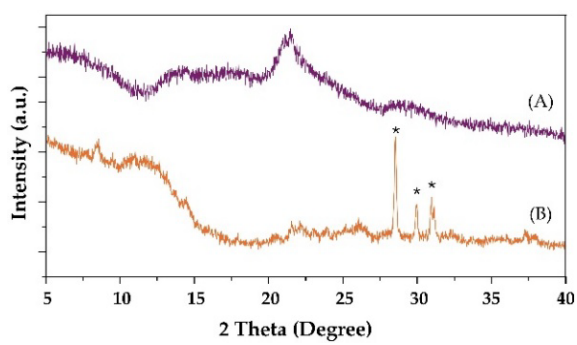

Figure 3: X-ray diffraction patterns of (A) commercial pectin (CP) and (B) watermelon pectin (WP) extracted via the steam explosion technique. The asterisks (*) indicate sharp crystalline reflections corresponding to the integrated mineral phases naturally present in the watermelon rind matrix.

This structure facilitates higher water accessibility and faster hydration rates compared to highly crystalline materials [37]. While the CP shows a relatively cleaner amorphous profile, the SE-extracted pectin displays a more diffused halo. This suggests that the intense mechanical disruption and rapid decompression during the steam explosion process effectively prevented the close packing of the pectic polysaccharides, resulting in a more disordered molecular architecture [10], [37]. This structural destabilization tracks consistently with thermal and hydrothermal pretreatments on complex biomass matrices, where high thermal-pressure parameters systematically break down the inter-linked cell wall components and induce partial macromolecular degradation, thereby fundamentally altering the amorphous-crystalline equilibrium and expanding the structural surface availability of the recovered biopolymer [38], [39]

Significantly, unlike the CP sample, the SE-extracted WP exhibits several distinct and sharp crystalline reflections superimposed on the amorphous background. The appearance of these sharp peaks at $2\theta = 28.5°$, 30.1°, and 31.6° suggests the presence of inorganic mineral salts. To definitively validate these structural forms and eliminate ambiguity, Energy-Dispersive X-ray Spectroscopy (EDS) and elemental mapping were conducted, with the quantitative profiling and microstructural distribution illustrated in Table 2 and Figure 4, respectively. The EDS spectra (Figure 4B) conclusively demonstrated the co-existence of major mineral-forming elements embedded inside the organic carbon-oxygen pectin infrastructure. As summarized in Table 2, the recovered WP matrix contains substantial concentrations of Potassium (K, 5.12 - 8.92 wt%), Sodium (Na, 0.15 - 0.54 wt%), Chlorine (Cl, 0.99 - 3.61 wt%), Calcium (Ca, 0.19 - 0.34 wt%), and Magnesium (Mg, 0.25 - 0.76 wt%) distributed alongside the carbon(C) and oxygen(O) backbones.

Table 2: Elemental composition of SE-extracted watermelon pectin (WP) derived from quantitative SEM-EDS profiling.

Element	Weight (wt%)*	Atomic (%)*
Carbon (C)	51.58 - 59.93	61.79 - 69.28
Oxygen (O)	31.88 -37.72	27.67 - 33.93
Potassium (K)	5.12 - 8.92	1.84 - 3.32
Chlorine (Cl)	0.99 - 3.61	0.39 - 1.48
Magnesium (Mg)	0.25 -0.76	0.15 - 0.44
Calcium (Ca)	0.19 - 0.34	0.06 - 0.12
Sodium (Na)	0.15- 0.54	0.08 - 0.25

*Note : Data represents the minimum and maximum values obtained across multiple spectrum mapping areas from the WP samples.

Crucially, the elemental mapping graphics (Figure 4C-I) reveal a deep structural insight regarding the distribution of these inorganic constituents. Rather than

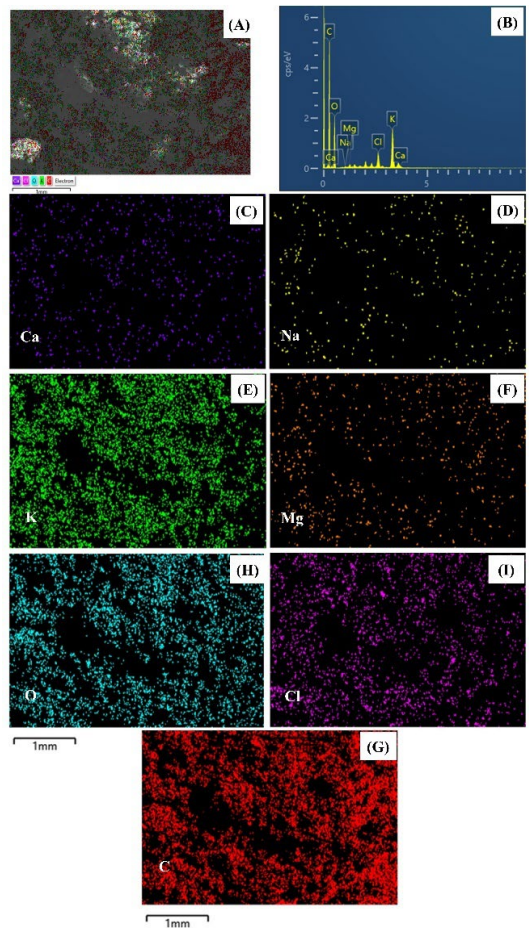

Figure 4 : SEM-EDS quantitative profile and elemental mapping analysis of the steam-exploded watermelon pectin (WP) (A) EDS layered image illustrating the co-localization of organic and inorganic phases, (B) EDS spectrum identifying the characteristic energy peaks of constituent elements, and (C-I) high-resolution elemental mapping configurations tracking the continuous microstructural distribution of calcium (Ca), sodium (Na), potassium (K), magnesium (Mg), oxygen (O), chlorine (Cl), and carbon (C) across the biopolymer framework.

existing as isolated superficial contaminants, all detected mineral elements are homogeneously integrated and continuously distributed throughout the organic pectic framework. This overlapping spatial arrangement provides strong chemical validation for the crystallographic indexation derived from XRD analysis.

Specifically, the sharp diffraction peak at $2\theta = 28.5°$ is verified by the prominent and uniform distribution of potassium(K) (Figure 4E) and Chlorine(Cl) (Figure 4I), confirming its identity as sylvite (KCl) [40], [41]. The reflection at 30.1° corresponds to the characteristic lattice plane of calcite ($CaCO_3$) (JCPDS : 88-1809), corroborated by the distinct co-localization of calcium (Figure 4C) alongside carbon (Figure 4G) and oxygen (Figure 4H) [42], [43], [44].

The presence of calcite in plant tissues is well established in the literature, since this crystalline phase naturally forms as a biomineral in the pericarps of various fruits and in leaf cystoliths [43], [45], [46]. These biomineralized calcite crystals are typically deposited within the cell wall compartments or intracellular spaces following cellular disruption [42], [47], which is consistent with our observed crystallographic identification of $CaCO_3$ in the watermelon peel matrix.

Furthermore, the sharp reflection at 31.6° aligns precisely with halite (NaCl), authenticated by the co-localization of sodium (Na) (Figure 4D) and chlorine (Cl) (Figure 4I) tracking across the exact microstructural layout of the pectin sheets [40]. In addition to the crystalline phases, the consistent detection of magnesium (Mg) (Figure 4F) across all investigated regions offers a valuable phytochemical explanation. Magnesium is inherently abundant in the green rind tissue of *Citrullus lanatus*, primarily serving as the central coordinating ion within the porphyrin rings of chlorophyll complexes [48], [49]. The absence of sharp, discrete Mg-containing crystalline peaks in the companion XRD patterns indicates that magnesium does not form independent mineral crystals. Instead, it remains bound in an amorphous complexed state or associated with the carboxylic groups of the galacturonic backbone, as supported by established pectin-cation binding studies [50], [51]. From a mechanistic standpoint, the integration of these distinct mineral phases (KCl, NaCl, and $CaCO_3$) is directly driven by the high-pressure steam explosion process. The sudden, explosive decompression violently ruptures the plant cell wall matrix, instantly solubilizing and mobilizing the intracellular mineral salts inherently present in the raw watermelon biomass[10], [52]. As the steam condenses and the pectic polysaccharides precipitate, these ions become entrapped and co-crystallize within the developing porous biopolymer network [51], [53], [54].

This structural encapsulation successfully accounts for the elevated ash content of 6.42 ± 0.15 %) observed in the WP compared to purified commercial pectin, which typically undergoes aggressive chemical washing with ash contents below 5% [7], [9]. Consequently, the retention of these naturally occurring mineral complexes within the amorphous pectin matrix yields a unique, integrated hybrid biopolymer with improved structural diversity and enhanced thermal stability without sacrificing its requisite hydration functionality [55], [56].

3.5. *Thermal analysis*

The thermal stability and phase transition behaviors of the extracted watermelon pectin (WP) and commercial pectin (CP) were evaluated using Thermogravimetric Analysis (TGA) and Differential Scanning Calorimetry (DSC). The resulting thermograms, illustrated in Figure 5 and Figure 6, provide critical insights into the structural integrity of the biopolymers, with the corresponding data summarized in Table 3.

3.5.1 Thermogravimetric analysis

The TGA/DTG thermograms illustrated in Figure 5 reveal a characteristic three-stage weight loss profile for both CP and WP, underscoring the structural complexity and thermal resilience of pectic polysaccharides. The initial loss occurring between 50 and 150 °C is attributed to the evaporation of adsorbed water and bound moisture, where WP exhibits a weight loss of 7.34% compared to 10.25% for CP. These values are consistent with literature limits of 10% or less for quality pectin, suggesting that the extraction and drying methods effectively manage the bound water within the pectin structure [35].

The second stage represents the major chemical degradation occurring in the range of 200 to 350 °C, which corresponds to the pyrolytic breakdown of the galacturonic acid backbone via decarboxylation, ester group loss, and alpha glycosidic scission [8], [57]. WP displays a maximum decomposition temperature of 253.05 °C, which is nearly identical to the 252.18 °C observed for CP. This similarity provides robust

Table 3: Thermal degradation and phase transition parameters of CP and SE-extracted WP derived from TGA and DSC analyses.

Sample	TGA					DSC			
	Stage 1		Stage 2		Residue at 550 °C (%)	Endothermic Peak		Exothermic Peak	
	Weight loss (%)	Tonset (°C)	Tmax (°C)	Weight loss (%)		Tpeak (°C)	ΔH (J/g)	Tpeak (°C)	ΔH (J/g)
CP	10.25	210.15	252.18	60.00	29.75	144.48	131.04	241.34	124.05
WP	7.34	212.30	253.05	48.83	43.83	135.85	168.72	243.48	35.04

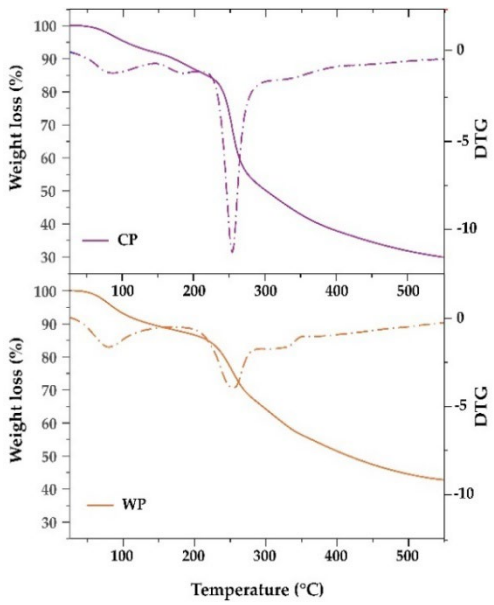

Figure 5: TGA and DTG thermograms of (A) commercial citrus pectin (CP) and (B) watermelon pectin (WP) extracted via the steam explosion technique.

evidence that the steam explosion process successfully preserves the inherent chemical integrity of the pectin backbone, as further corroborated by DSC and XRD findings [8].

Significantly, WP exhibits a substantially higher char residue at 550 °C of 43.83% compared to 29.75% for the CP sample. This elevated residue is directly linked to the 6.42% ash content originating from natural minerals in the watermelon rind, such as potassium and magnesium, which act as a thermal barrier and enhance stability at elevated temperatures [8], [35]. This three-stage pattern aligns with reported pectin behaviors influenced by botanical origin and degree of esterification [58]. Collectively, these profiles highlight the role of the eco-friendly SE process in yielding a mineral-enriched biopolymer ideal for high-temperature food applications, providing a solid foundation for future kinetic analysis of activation energy [10].

3.5.2. Differential scanning calorimetry

The DSC thermograms (Figure 6) complement the TGA findings by revealing energetic changes during thermal transitions [58], [59]. Both CP and WP exhibit a broad endothermic peak at 80 - 120 °C, which is associated with the enthalpy of vaporization required for the dehydration of the hydrophilic polysaccharide network [59], [60]. Specifically, WP shows an endothermic peak temperature of 135.85 °C with a corresponding enthalpy of 168.72 J/g. This higher peak temperature and energy requirement compared to the 119.25 °C and 131.04 J/g observed for CP indicates that water molecules within the WP matrix possess stronger interactions with functional groups or integrated minerals co-extracted during the steam explosion process [8], [35]. The oxidative thermal degradation and subsequent charring of the pectic chains are represented by a sharp exothermic peak appearing between 240 and 260 °C [58], [59]. For the WP sample, this peak aligns precisely at 241.45 °C,

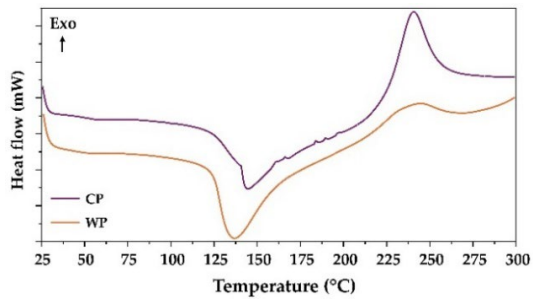

Figure 6: DSC thermograms of commercial pectin (CP) and watermelon pectin (WP) extracted via the steam explosion technique.

which correlates with the maximum decomposition temperature found in the TGA data.

Notably, the exothermic enthalpy for WP is 35.04 J/g, which is significantly lower than the 124.05 J/g recorded for CP. This difference reflects variations in molecular architecture and the presence of non-volatile mineral components that influence the overall energy release during polymer breakdown [8], [57]. The near-identical degradation temperatures between WP and CP demonstrate that steam explosion effectively preserves the fundamental structural integrity of the pectic backbone [8]. These findings suggest that watermelon rind pectin possesses robust thermal stability suitable for high-temperature food processing applications such as pasteurization or bakery production [8], [10].

Collectively, the thermal analysis validates the steam explosion technique as an efficient and environmentally benign method for yielding a mineral-enriched biopolymer with comparable thermal characteristics to commercial standards [58].

4 Conclusions

This research successfully demonstrates the efficacy of the steam explosion (SE) technique as an efficient method that is potentially greener than conventional acid extraction, owing to the reduced use of harsh acids, for obtaining high-quality pectin from watermelon rinds. The SE-extracted pectin (WP) achieved a yield of 3.41 ± 0.13% with a degree of esterification (DE) of 37.42 ± 1.92%, effectively classifying it as low-methoxyl pectin (LMP). Comprehensive characterization via FTIR, SEM-EDS, XRD, and thermal analysis (TGA/DSC) revealed distinct structural and functional advantages. While FTIR confirmed the preservation of the essential galacturonic acid backbone, XRD and SEM-EDS mapping analyses highlighted a unique hybrid morphology, which consists of a predominantly amorphous pectic matrix integrated with crystalline mineral phases of Sylvite (KC), Calcite ($CaCO_3$), and Halite (NaCl). This integrated mineral structure, resulting from the rapid decompression of the cell wall matrix, provides a distinctive structural profile over commercial citrus pectin through its inherent multi-elemental retention property. Furthermore, the WP exhibited robust thermal stability and high residue content, indicating its suitability for high-temperature industrial applications. The valorization of watermelon waste through steam explosion not only reduces the chemical footprint by minimizing mineral-stripping acid treatments but also yields a functional biopolymer with co-extracted and integrated crystalline mineral phases. These findings provide a scientific foundation for utilizing watermelon-derived pectin in sustainable food and pharmaceutical applications, contributing to both environmental sustainability and the circular economy.

Acknowledgments

We also extend our appreciation to the Department of Chemistry, Faculty of Science and Digital Innovation, Thaksin University, Phatthalung campus, for their expert chemical suggestions and support throughout this research, as well as to the Centre of Excellence for Agricultural Innovation and Bioproducts of Thaksin University.

Author Contributions

T.B.: data analysis, formal analysis, writing-original draft preparation; N.N.: investigation, methodology; K.M.: investigation, methodology; S.S.: investigation, methodology; V.B.: data curation, visualization; N.P.: conceptualization, supervision, project administration, funding acquisition, writing-reviewing and editing. All authors have read and agreed to the published version of the manuscript.

Conflicts of Interest

The authors declare no conflict of interest.

Declaration of generative AI and AI-assisted technologies in the writing process

The authors utilized Gemini to enhance the language and readability of the manuscript. After using this tool, the authors reviewed and edited the content as needed and take full responsibility for the final version.

References

[1] A. Gorgulu and Y. F. Gorgulu, “Production of sustainable food ingredients from watermelon wastes using drum-drying,” *Journal of Food Process Engineering*, vol. 48, no. 1, art. no. e70040, Jan. 2025, doi: 10.1111/jfpe.70040.

[2] S. Badr, M. El-Waseif, and M. Ghaly, “Effect of addition watermelon rind powder on quality

criteria and microbial aspects of beef burger patties during frozen storage periods," *Journal of Food and Dairy Sciences*, vol. 9, no. 6, pp. 177-187, Jun. 2018, doi: 10.21608/jfds.2018.35852.

[3] S. Pradhan, B. Yuzer, Y. Bicer, G. McKay, and T. Al-Ansari, "Hydrogen gas and biochar production from kitchen food waste through dark fermentation and pyrolysis," *Frontiers in Chemical Engineering,* vol. 6, art. no. 1450151, Nov. 2024, doi: 10.3389/fceng.2024.1450151.

[4] X. Jin, Y. Han, and Q. Sun, "Serial extraction of pectin and polyphenols from watermelon rind for use in strawberry preservation film," *Journal of Food Science*, vol. 90, no. 4, art. no. e70216, Apr. 2025, doi: 10.1111/1750-3841.70216.

[5] Y.-S. Cheng et al., "Recent situation and progress in biorefining process of lignocellulosic biomass: Toward green economy," *Applied Science and Engineering Progress,* vol. 13, no. 4, pp. 299-311, Oct. 2020, doi: 10.14416/j.asep.2020.08.002.

[6] E. J. Panakkal et al., "Influence of sulfuric acid pretreatment and inhibitor of sugarcane bagasse on the production of fermentable sugar and ethanol," *Applied Science and Engineering Progress*, vol. 15, no. 1, Jul. 2021, doi: 10.14416/j.asep.2021.07.006.

[7] D. Mamiru and G. Gonfa, "Extraction and characterization of pectin from watermelon rind using acetic acid," *Heliyon*, vol. 9, no. 2, art. no. e13525, Feb. 2023, doi: 10.1016/j.heliyon.2023.e13525.

[8] J. Perez, K. Gomez, and L. Vega, "Optimization and preliminary physicochemical characterization of pectin extraction from watermelon rind (*Citrullus lanatus*) with citric acid," *International Journal of Food Science*, vol. 2022, pp. 1-10, Jan. 2022, doi: 10.1155/2022/3068829.

[9] N. Saiharini and A. Padmaja, "Studies on nutrient and phytochemical composition and assessment of in vitro antioxidant and enzyme inhibitory properties of watermelon fruit by-products," *Annals of Phytomedicine,* vol. 11, no. 1, Jul. 2022, doi: 10.54085/ap.2022.11.1.48.

[10] M. Gavahian, G. N. Mathad, R. Pandiselvam, J. Lin, and D.-W. Sun, "Emerging technologies to obtain pectin from food processing by-products: A strategy for enhancing resource efficiency," *Trends in Food Science & Technology*, vol. 115, pp. 42-54, Sep. 2021, doi: 10.1016/j.tifs.2021.06.018.

[11] C. Ma et al., "Principle and application of steam explosion technology in modification of food fiber," *Foods*, vol. 11, no. 21, Art. no. 3370, Oct. 2022, doi: 10.3390/foods11213370.

[12] L. N. Jiang, J. J. Shang, L. B. He, and J. M. Dan, "Comparisons of microwave-assisted and conventional heating extraction of pectin from seed watermelon peel," *Advanced Materials Research,* vol. 550-553, pp. 1801–1806, Jul. 2012, doi: 10.4028/www.scientific.net/AMR.550-53.1801.

[13] M. S. Rahman, S. S. Khan, M. W. Ahmed, M. E. Jony, p. C. Das, and M. B. Uddin, "Extraction of pectin from Elephant Apple and Pomelo fruit peels: Valorization of fruit waste towards circular economy," *Food Chemistry Advances*, vol. 3, art. no. 100544, Dec. 2023, doi: 10.1016/j.focha.2023.100544.

[14] I. L. G. Lekhuleni, T. E. Kgatla, M. E. Mashau, and A. I. O. Jideani, "Physicochemical properties of South African prickly pear fruit and peel: Extraction and characterisation of pectin from the peel," *Open Agriculture*, vol. 6, no. 1, pp. 178-191, Mar. 2021, doi: 10.1515/opag-2021-0216.

[15] N. H. Hasem, S. F. Z. Mohamad Fuzi, F. Kormin, M. F. Abu Bakar, and S. F. Sabran, "Extraction and partial characterization of durian rind pectin," *IOP Conference Series: Earth and Environmental Science*, vol. 269, no. 1, art. no. 012019, Jul. 2019, doi: 10.1088/1755-1315/269/1/012019.

[16] M. Duggal, D. p. Singh, S. Singh, S. Khubber, M. Garg, and M. Krishania, "Microwave-assisted acid extraction of high-methoxyl kinnow (*Citrus reticulata*) peels pectin: Process, techno-functionality, characterization and life cycle assessment," *Food Chemistry: Molecular Sciences,* vol. 9, art. no. 100213, Dec. 2024, doi: 10.1016/j.fochms.2024.100213.

[17] S. H. Jong, N. Abdullah, and N. Muhammad, "Optimization of low-methoxyl pectin extraction from durian rinds and its physicochemical characterization," *Carbohydrate Polymer Technologies and Applications,* vol. 5, art. no. 100263, Jun. 2023, doi: 10.1016/j.carpta.2022.100263.

[18] M. Zioga, E. Tsouko, S. Maina, A. Koutinas, I. Mandala, and V. Evageliou, "Physicochemical and rheological characteristics of pectin extracted from renewable orange peel employing conventional and green technologies," *Food hydrocolloids*, vol. 132, art. no. 107887, Nov. 2022, doi: 10.1016/j.foodhyd.2022.107887.

[19] Y. Yu et al., "Differences in physicochemical properties of pectin extracted from pomelo peel with different extraction techniques," *Scientific Reports,* vol. 14, art. no. 9182, Apr. 2024, doi: 10.1038/s41598-024-59760-7.

[20] I. Santiago-Gomez et al., "Pectin extraction process from cocoa pod husk (*Theobroma cacao* L.) and characterization by Fourier Transform Infrared Spectroscopy," *ChemEngineering*, vol. 9, no. 2, art. no. 25, Feb. 2025, doi: 10.3390/chemengineering9020025.

[21] D. A. Mendez, M. J. Fabra, L. Gomez-Mascaraque, A. Lopez-Rubio, and A. Martinez-Abad, "Modelling the extraction of pectin towards the valorisation of watermelon rind waste," *Foods*, vol. 10, no. 4, art. no. 738, Mar. 2021, doi: 10.3390/foods10040738.

[22] Z. Wu et al., "Physicochemical and functional properties of *Lycium ruthenicum* pectin by different extraction methods," *Frontiers in Nutrition,* vol. 9, art. no. 946606, Aug. 2022, doi: 10.3389/fnut.2022.946606.

[23] A. Fidalgo et al., "Eco-friendly extraction of pectin and essential oils from orange and lemon peels," *ACS Sustainable Chemistry & Engineering,* vol. 4, no. 4, pp. 2243-2251, Apr. 2016, doi: 10.1021/acssuschemeng.5b01716.

[24] J. González-Rivera et al., "Novel configurations for a citrus waste based biorefinery: From solventless to simultaneous ultrasound and microwave assisted extraction," *Green chemistry,* vol. 18, no. 24, pp. 6482-6492, 2016, doi: 10.1039/C6GC02200F.

[25] D. Panwar, P. S. Panesar, and H. K. Chopra, "Green extraction of pectin from *Citrus limetta* peels using organic acid and its characterization," *Biomass Conversion and Biorefinery*, vol. 14, no. 1, pp. 159–171, Jan. 2024, doi: 10.1007/s13399-021-02127-z.

[26] S.A. Rezzoug, Z. Maache-Rezzoug, F. Sannier, and K. Allaf, "A thermomechanical preprocessing for pectin isolation from orange peel with optimisation by response surface methodology," *International Journal of Food Engineering,* vol. 4, no. 1, art. no. 6, Jan. 2008, doi: 10.2202/1556-3758.1183.

[27] T. Mada, R. Duraisamy, and F. Guesh, "Optimization and characterization of pectin extracted from banana and papaya mixed peels using response surface methodology," *Food Science & Nutrition*, vol. 10, no. 4, pp. 1222-1238, Apr. 2022, doi: 10.1002/fsn3.2754.

[28] S. Susanti, A. M. Legowo, N. Nurwantoro, S. Silviana, and F. Arifan, "Comparing the chemical characteristics of pectin isolated from various Indonesian fruit peels," *Indonesian Journal of Chemistry,* vol. 21, no. 4, pp. 1057-1064, Apr. 2021, doi: 10.22146/ijc.59799.

[29] M. Saraha, M. F. Hisham, M. Rizki, and R. Erwinda, "Effect of power and time in pectin production from cocoa pod husk using microwave-assisted extraction technique," *International Journal of Renewable Energy Development,* vol. 9, no. 1, pp. 125-130, Mar. 2020, doi: 10.14710/ijred.9.1.125-130.

[30] N. Z. A. Daud, B. N. M. Said, F. Ja'afar, H. M. Yasin, E. Kusrini, and A. Usman, "pH-dependent yield and physicochemical properties of pectin isolated from *Citrus Maxima*," *International Journal of Technology,* vol. 10, no. 6, pp. 1131-1138, Nov. 2019, doi: 10.14716/ijtech.v10i6.3595.

[31] M. Spinei and M. Oroian, "Microwave-assisted extraction of pectin from grape pomace," *Scientific Reports*, vol. 12, no. 1, art. no. 12722, Jul. 2022, Jul. 2022, doi: 10.1038/s41598-022-16858-0.

[32] Z. Yuan, J. Yan, Q. Zhang, J. Zheng, and A. Hu, "Effects of steam explosion on physicochemical, functional and structural properties of soluble dietary fiber from pomelo peel," *International Journal of Food Engineering,* vol. 19, no. 10, pp. 457-465, Oct. 2023, doi: 10.1515/ijfe-2023-0099.

[33] Y. Xing et al., "Structural, physicochemical and functional properties of dietary fibers from tea residue modified by steam explosion," *Frontiers in Sustainable Food Systems*, vol. 7, art. no. 1326102, Jan. 2024, doi: 10.3389/fsufs.2023.1326102.

[34] M. L. Fishman, P. N. Walker, H. K. Chau, and A. T. Hotchkiss, "Flash extraction of pectin from orange albedo by steam injection," *Biomacromolecules*, vol. 4, no. 4, pp. 880-889, Jul. 2003, doi: 10.1021/bm020122e.

[35] P. P. Shameena Beegum, V. R. Sagar, A. Kar, E. Varghese, S. Singh, and A. Pongener, "Optimization of pectin extraction from watermelon rind and characterization of the extracted pectin," *Journal of Agricultural Engineering (India)*, vol. 61, no. 6, pp. 862–875, Dec. 2024, doi: 10.52151/jae2024616.1900.

[36] E. Piacenza et al., "Cross-linked natural IntegroPectin films from citrus biowaste with intrinsic antimicrobial activity," *Cellulose*, vol. 29, no. 10, pp. 5779-5802, Jul. 2022, doi: 10.1007/s10570-022-04627-1.

[37] M. F. Kurniawan, D. Setyawan, and D. M. Hariyadi, "Pectin red dragon fruit peel pectin-based microspheres for oral quercetin delivery: Characterization, stability study, digestion resistance, and cytotoxicity against HeLa cells," *Science and Technology Indonesia*, vol. 10, no. 4, pp. 1049-1073, Oct. 2025, doi: 10.26554/sti. 2025.10.4.1049-1073.

[38] B. Saha, M. Khwairakpam, and A. S. Kalamdhad, "Thermal pre-treatment - A prerequisite for the reduction of hydrolysis stage during anaerobic digestion of *Ageratum conyzoides*," *Materials Science for Energy Technologies*, vol. 4, pp. 34-45, Dec. 2021, doi: 10.1016/j.mset.2020.12.002.

[39] B. Saha et al., "Optimising biogas production from *Parthenium hysterophorus* biomass through thermal pretreatment and batch anaerobic digestion," *Fermentation*, vol. 12, no. 3, art. no. 135, Mar. 2026, doi: 10.3390/fermentation 12030135.

[40] C. E. Meng et al., "Mineral composition, crystallinity and dielectric evaluation of bamboo salt, Himalaya salt, and Ba'kelalan salt content," *Heliyon*, vol. 10, no. 1, art. no. e23847, Jan. 2024, doi: 10.1016/j.heliyon.2023.e23847.

[41] Y. Wang, H. Wu, Z. Sárossy, C. Dong, and p. Glarborg, "Release and transformation of chlorine and potassium during pyrolysis of KCl doped biomass," *Fuel*, vol. 197, pp. 422-432, Jun. 2017, doi: 10.1016/j.fuel.2017.02.046.

[42] H. Barhom et al., "Biological Kerker effect boosts light collection efficiency in plants," *Nano Letters,* vol. 19, no. 10, pp. 7062-7071, Oct. 2019, doi: 10.1021/acs.nanolett.9b02540.

[43] E. N. Ikkonen et al., "Identification and distribution of biominerals in pericarp of *Boraginaceae* fruits," *Russian Journal of Plant Physiology,* vol. 72, no. 4, art. no. 125, Aug. 2025, doi: 10.1134/S1021443725601454.

[44] P. Paramita et al., "Sol-gel based synthesis and biological properties of zinc integrated nano bioglass ceramics for bone tissue regeneration," *Journal of Materials Science: Materials in Medicine,* vol. 32, no. 1, art. no. 5, Jan. 2021, doi: 10.1007/s10856-020-06478-3.

[45] A. Gal, V. Brumfeld, S. Weiner, L. Addadi, and D. Oron, "Certain biominerals in leaves function as light scatterers," *Advanced Materials*, vol. 24, no. 10, pp. 1283-1286, Mar. 2012, doi: 10.1002/adma.201104548.

[46] A. Gal et al., "Plant cystoliths: A complex functional biocomposite of four distinct silica and amorphous calcium carbonate phases," *Chemistry – A European Journal,* vol. 18, no. 33, pp. 10262-10270, Aug. 2012, doi: 10.1002/chem.201201111.

[47] A. Gal, S. Weiner, and L. Addadi, "The stabilizing effect of silicate on biogenic and synthetic amorphous calcium carbonate," *Journal of the American Chemical Society,* vol. 132, no. 38, pp. 13208-13211, Sep. 2010, doi: 10.1021/ja106883c.

[48] T. Bohn, T. Walczyk, S. Leisibach, and R. F. Hurrell, "Chlorophyll-bound magnesium in commonly consumed vegetables and fruits: Relevance to magnesium nutrition," *Journal of Food Science,* vol. 69, no. 9, pp. S347–S350, Dec. 2004, doi: 10.1111/j.1365-2621.2004.tb09947.x.

[49] C. Hermans, G. N. Johnson, R. J. Strasser, and N. Verbruggen, "Physiological characterisation of magnesium deficiency in sugar beet: Acclimation to low magnesium differentially affects photosystems I and II," *Planta*, vol. 220, no. 2, pp. 344-355, Dec. 2004, doi: 10.1007/ s00425-004-1340-4.

[50] A. Malovikova, M. Rinaudo, and M. Milas, "Comparative interactions of magnesium and calcium counterions with polygalacturonic acid," *Biopolymers*, vol. 34, no. 8, pp. 1059-1064, Aug. 1994, doi: 10.1002/bip.360340809.

[51] M. Celus, C. Kyomugasho, A. M. Van Loey, T. Grauwet, and M. E. Hendrickx, "Influence of pectin structural properties on interactions with divalent cations and its associated functionalities," *Comprehensive Reviews in Food Science and Food Safety,* vol. 17, no. 6, pp. 1576-1594, Nov. 2018, doi: 10.1111/1541-4337.12394.

[52] Y. Liang et al., "Extraction of pectin from passion fruit peel: Composition, structural characterization and emulsion stability," *Foods*, vol. 11, no. 24, art. no. 3995, Dec. 2022, doi: 10.3390/foods11243995.

[53] P. Sriamornsak, "Application of pectin in oral drug delivery," *Expert Opinion on Drug Delivery*, vol. 8, no. 8, pp. 1009-1023, Aug. 2011, doi: 10.1517/17425247.2011.584867.

[54] T. E. L. Douglas et al., "Pectin-bioactive glass self-gelling, injectable composites with high antibacterial activity," *Carbohydrate polymers,* vol. 205, pp. 427-436, Feb. 2019, doi: 10.1016/j.carbpol.2018.10.061.

[55] J. Cao, M. N. Corstens, and K. Schroën, "Enhanced thermal stability of potato protein-pectin emulsions: Synergistic effects of bulk and interfacial properties," *LWT - Food Science and Technology*, vol. 241, art. no. 119050, Feb. 2026, doi: 10.1016/j.lwt.2026.119050.

[56] J. Song, V. Malathong, and C. R. Bertozzi, "Mineralization of synthetic polymer scaffolds: A bottom-up approach for the development of artificial bone," *Journal of the American Chemical Society*, vol. 127, no. 10, pp. 3366–3372, Mar. 2005, doi: 10.1021/ja043776z.

[57] C. Gómez Vargas et al., "Pectin obtention from agroindustrial wastes of *Malus domestica* using green solvents (citric acid and natural deep eutectic solvents): Chemical, thermal, and rheological characterization," *Frontiers in Chemistry,* vol. 12, Art. no. 1504582, Jan. 2025, doi: 10.3389/fchem.2024.1504582.

[58] M. Jimenez et al., "Matrices of native and oxidized pectin and ferrous bisglycinate and their in vitro behavior through gastrointestinal conditions," *Colloids and Interfaces*, vol. 7, no. 2, art. no. 35, Apr. 2023, doi: 10.3390/colloids 7020035.

[59] N. Karaki, A. Aljawish, L. Muniglia, C. Humeau, and J. Jasniewski, "Physicochemical characterization of pectin grafted with exogenous phenols," *Food hydrocolloids.*, vol. 60, pp. 486-493, Oct. 2016, doi: 10.1016/j. foodhyd.2016.04.004.

[60] M. Renteria-Ortega et al., "Characterization and applications of the pectin extracted from the peel of *Passiflora tripartita* var. *mollissima*," *Membranes*, vol. 13, no. 9, art. no. 797, Sep. 2023, doi: 10.3390/membranes13090797.